

Numerical study on the flow features of U-beam inertial separator*

CHEN Li-hua (陈丽华)[†], FAN Jian-ren (樊建人), CEN Ke-fa (岑可法)

(College of Mechanical and Energy Engineering, Zhejiang University, Hangzhou 310027, China)

[†]E-mail: mecelh@cmee.zju.edu.cn

Received May 6, 2002, Revision accepted July 29, 2002

Abstract: Detailed parametric study of three-dimensional gas-particle multiphase flow characteristics in U-beam tube bundle inertial separators was conducted by numerical simulation. The carrier phase was treated in the Eulerian frame, the particles were tracked in the Lagrangian frame, and particle-wall collision was considered. Simulation carried out at different inflow rate and mass loading ratios revealed the pressure losses in the separators, velocity field of the gas phase, and the trajectories of particles. The study results revealed the multiphase flow-dynamic features of the separators, and the relationship between separator pressure losses and different inlet velocity. The numerical simulation can provide basis both for optimal design of impacting-inertial separator used in circulating fluidized bed boiler; and for study of gas-particle multiphase circumfluence flow.

Key word: U-beam inertial separator, Numerical simulation, Dynamic features

Document code: A

CLC number: TK229.66

INTRODUCTION

Circulating fluidized bed (CFB) combustion is a most promising clean coal technique that has received worldwide attention. A main feature of CFB boilers is the undelayed recycling of solid, coal and sorbant particulates in an external loop. Separators, required to separate the solid particulates from the offgas leaving the reactor of the CFB, play an important role in the external solids recycling loop. Its workstation greatly affects the combustion and desulphazation of the CFB system.

Very recently inertial separator was proposed because of its low thermal inertial, simple construction and low cost (Cen et al., 1998; De et al., 1999; Baskakov et al., 2000). The inertial separator consists of tube bundles of different shapes and arranged staggered or in line. In inertial separators, the gas-solid suspension passes through a series of obstacles and undergoes sudden changes in the flow direction. Because of their inertia, solid particles tend to retain their origin movement direction, which makes the particles being separated from, instead of following, the flow stream around the collecting object. Most of the particles are separated from the gas flow stream after several impingements on the

impactors and repeated changes in direction. The impactor shape and its arrangement affect the separation efficiency significantly.

In this study, the inertial separator consisted of four rows of impact U-beam tube (Fig. 1) arranged staggered in the offgas flow direction. The inlet velocity of the gas-particles suspension flow is from 2 m/s to 10 m/s. The particles used in this study were quartz particle with Sauter diameter of 260 μm .

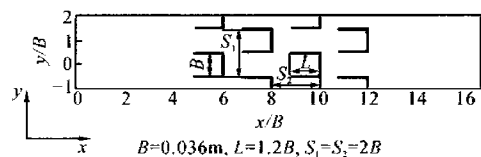


Fig. 1 Schematic of U-beam inertial separator and solution domain on x-y profile

NUMERICAL MODEL

In the case of gas-particle suspension flow, Lagrangian formulation with the equations of motion chosen for the particulate phase while the Eulerian approach used to simulate the continuous phase. (Huber et al., 1998; Zha et al., 2000)

* Project supported by the Zhejiang Provincial Natural Science Foundation of China (No. 500065)

Eulerian formulation for the gas

For a steady, fully developed turbulent flow, if the volume fraction of the solid particle is very small, the modeled transport equations in Cartesian coordinates can be written as

$$\left[\frac{\partial}{\partial x}(\rho(U\phi)) + \frac{\partial}{\partial y}(\rho(V\phi)) \right] - \left[\frac{\partial}{\partial x}(\Gamma_{\phi, \text{eff}} \frac{\partial \phi}{\partial x}) + \frac{\partial}{\partial y}(\Gamma_{\phi, \text{eff}} \frac{\partial \phi}{\partial y}) \right] = S_{\phi} \quad (1)$$

The two-equation turbulence model (k - ϵ model) is used to simulate turbulence transport effects. The particular expression for $\Gamma_{\phi, \text{eff}}$ and S_{ϕ} pertaining to each dependent variable ϕ are summarized in Table 1, with the appropriate empirical constants listed (Fan et al., 1997a). The finite-volume differential method is used to solve the governing equations, with boundary conditions.

Table 1 Diffusion and source terms

Parameter(ϕ)	Diffusion($\Gamma_{\phi, \text{eff}}$)	Source(S_{ϕ})
1	0	0
U	$\mu_{\text{eff}} \left[-\frac{\partial p}{\partial x} + \frac{\partial}{\partial x}(\mu_{\text{eff}} \frac{\partial U}{\partial x}) + \frac{\partial}{\partial y}(\mu_{\text{eff}} \frac{\partial V}{\partial x}) \right]$	
V	$\mu_{\text{eff}} \left[-\frac{\partial p}{\partial y} + \frac{\partial}{\partial x}(\mu_{\text{eff}} \frac{\partial U}{\partial y}) + \frac{\partial}{\partial y}(\mu_{\text{eff}} \frac{\partial V}{\partial y}) \right]$	
k	$\frac{\mu_{\text{eff}}}{\sigma_k}$	$G_k - \rho \epsilon$
ϵ	$\frac{\mu_{\text{eff}}}{\sigma_{\epsilon}}$	$C_1 G_k \frac{\epsilon}{k} - C_2 \rho \frac{\epsilon^2}{k}$

Lagrangian formulation for the particles

Consider the particle momentum equation for a single particle in the Lagrangian framework:

$$m_p \frac{d\mathbf{v}_p}{dt} = C_D \rho_g A_p \frac{|\mathbf{v}_g - \mathbf{v}_p|}{2} (\mathbf{v}_g - \mathbf{v}_p) + m_p \mathbf{g} \quad (2)$$

$$\frac{d\mathbf{r}_p}{dt} = \mathbf{v}_p \quad (3)$$

Eq. (2) is simply an expression for Newton's second law of motion for an individual particle and subjects to the specification of particle velocity. Subscript g means gas and p means particle. Empirical data were being used to fit the drag curve over a wide range of particles Reynolds number.

$$C_D = \frac{24}{Re_p} [1 + 0.15(Re_p)^{0.687}] \quad (Re_p < 1000)$$

$$C_D = 0.44 \quad (Re_p \geq 1000) \quad (4)$$

$$Re_p = \frac{\rho_g |\mathbf{v}_g - \mathbf{v}_p| d_p}{\mu}$$

Eq. (3) is subject to the specification of particle location. The fourth-order adaptive step size Runge-Kutta scheme is used to solve Eq. (2) and Eq. (3).

In this study, a stochastic particle dispersion model (Fan et al., 1997 b) is employed to determine the motion of the particles in the turbulent flow. Taking into account the effect of the turbulent flow of the gas on the particle motion, instantaneous gas velocity \mathbf{v}_g is expressed by the time-averaged velocity \mathbf{V}_g calculated from Eq. (1), and the fluctuating velocity \mathbf{v}_g' , $\mathbf{v}_g = \mathbf{V}_g + \mathbf{v}_g'$. Random Fourier series simulate the gas phase fluctuating velocity \mathbf{v}_g' in a particular eddy, i. e., the components of \mathbf{v}_g' may be expressed as

$$v_{gj}' = \sum_{i=1}^n R_j V_{mij} \cos(\omega_i t - R_{j+1} \alpha_i^j) \quad (j = x, y, z) \quad (5)$$

Where the random variables R_j and R_{j+1} are sampled from a uniform probability distribution between 0 and 1. α is the initial fluctuating phase velocity, and the frequency ω_i is picked from a Gaussian distribution with a standard deviation of unity. For the incompressible isotropic turbulent flow field, the fluctuating amplitude V_{mij} can be given as $V_{mij} = \left(\int_0^{\infty} E(K) dK \right)^{1/2}$ where $E(K)$ is the energy spectrum, and K is the wave number. Furthermore, a particle is assumed interact with an eddy for certain period of time, which is the minimum of either the eddy lifetime or the transit time. In the present work, 40 particle trajectories are calculated in each of the 400 starting locations uniformly distributed over the inlet plane of the calculation domain, for a total of 16 000 particle trajectories calculated.

Impact and rebound phenomenon of particles

Particle rebound characteristics had been studied experimentally (Grant et al., 1975). The change in particle momentum due to impact is found to be mainly a function of the particle impact velocity W and its incidence angel β . The following empirical relationships between rebound and impact restitution ratios are used in trajectories calculation, where subscript N means normal to the wall and T tangent to the wall, 1 and 2 refer to the conditions before and after impact, respectively.

$$W_{N_2}/W_{N_1} = 1.0 - 0.4159\beta_1 - 0.4994\beta_1^2 + 0.292\beta_1^3 \quad (6)$$

$$W_{T_2}/W_{T_1} = 1.0 - 2.12\beta_1 + 3.0775\beta_1^2 - 1.1\beta_1^3 \quad (7)$$

RESULTS AND DISCUSSION

Numerical result of gas phase

Fig. 2 shows the gas velocity vectors predicted using the procedure described above when the inlet velocity is 4 m/s. the velocity field proves to be similarly when inlet velocity is 2 m/s and 10 m/s. The gas turns sharply before the U-beam impactor where the slip velocity between gas and particles becomes higher. The gas velocity decreases rapidly before the U-beam impactor and back-flow exits at the back of the impactor. The lower half of Fig. 2 describes the variation of velocity across the flow field. The contour plots in gray scale shows the magnitude of velocity from small scale to large corresponding to the color from black to white.

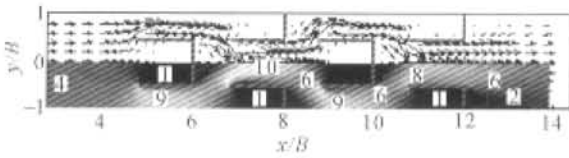


Fig. 2 Gas velocity vector and contour on x - y profile (u₀ = 4 m/s)

Fig. 3 presents the pressure contour of U-beam tube bundles (u₀ = 4 m/s). In order to increase the sensitivity of the pressure correction equation, the value of pressure used in Eq. (1) was the real pressure minus the outlet pressure.

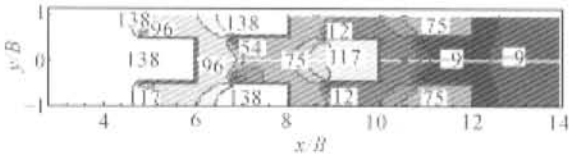


Fig. 3 Pressure contour on x - y profile (u₀ = 4 m/s)

When the inlet velocity increased the pressure losses increased rapidly. After the pressure loss Δp is transformed to dimensionless number (named resistance coefficient) C_p = 2Δp/ρu₀² with the offgas inlet kinematics energy (ρ is the

density of offgas). Fig. 4 shows the variation tendency of C_p and pressure loss with increase of inlet velocity. The resistance coefficient corresponding to u₀ = 4 m/s is the lowest at four points when inlet velocity increases from 2 m/s to 10 m/s. It means that we should not just cut-off the inlet velocity when asked to reduce the pressure loss.

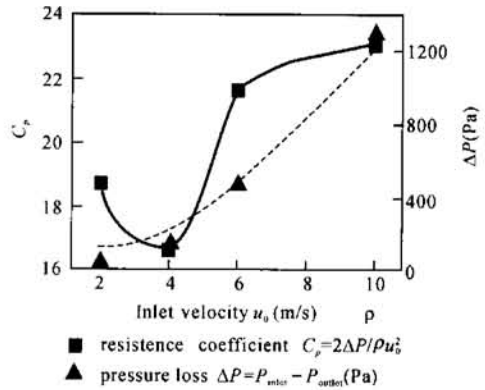


Fig. 4 Relationship of the pressure loss Δp and resistance coefficient c_p with the inlet velocities u₀

Particle trajectory analysis

Free stream velocity and the property of the particle affect the particle trajectories. Fig. 5 shows typical particle trajectories from the same altitude of U-beam separator in vertical direction (z direction). The Fig. 5 (a) and Fig. 5 (b) illustrate how the inertial force's influence the particle separation while the Fig. 5 (c) show the influence of gravity on the particle separation. The Fig. 5 (a) and (b) show that particles keep their origin moving direction because of inertia and are separated mostly by the first and second rows of impactors. We found that gravity played an important role in the separation, especially of larger particles. In other words, many particles enter into the low-velocity field of U-beam tube and then falling to be separated.

Fig. 5 also shows the typical trajectories of different size particle starting from the same station. The particle movement differs with its mass. From Fig. 5 we could see particle size affect the separation efficiency. Generally the larger the particle size, the easier it is separated. On the other hand, with increasing particle size to a extent, particles may escape from the separator

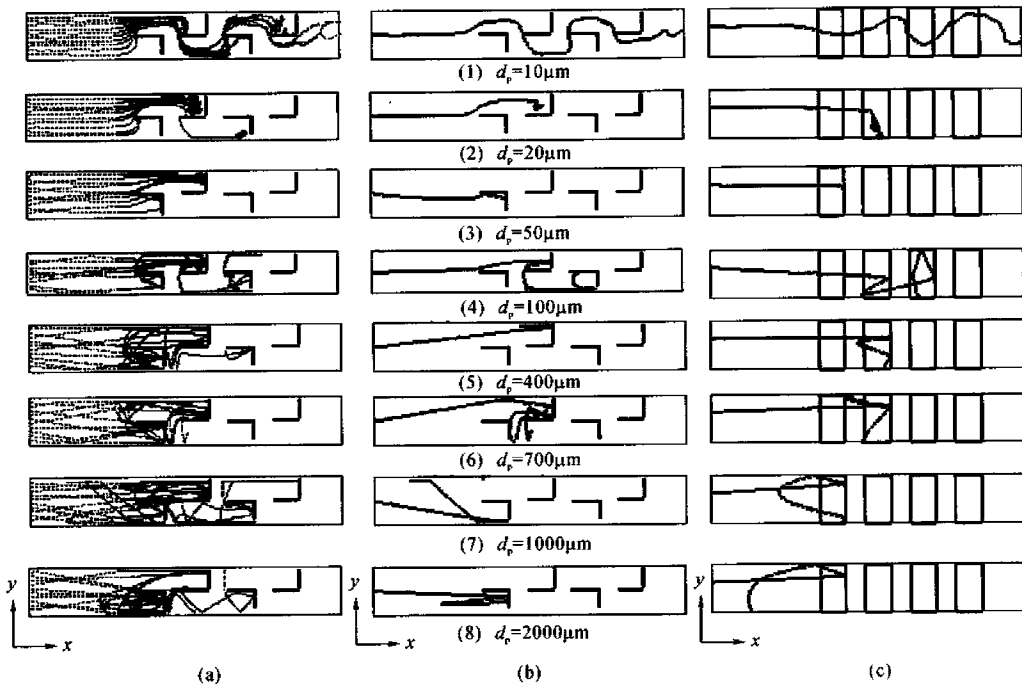


Fig. 5 Particle parcel trajectories from the same station and of different particle sizes on $x-y$ profile (a); single particle trajectory from the same station and of different sizes on $x-y$ profile (b); on $x-z$ profile (c)

because its greater inertia may help it rebound out of the tubes.

CONCLUSIONS

Our numerical simulation of the flow dynamics features of the staggered U-beam tube bundles inertial separator and statistical analysis of the trajectories of particles in the tubes, led to the conclusions: The gas changes its flow direction suddenly because of obstruction from the U-beam tube. At the same time the particles are separated as they try to keep to their original moving direction. The zone between the U-beam tube boundaries contributes to separation of the particles. If particles entered they are separated mostly except that some may rebound to leave the zone. The erosion of the inertial separator might be a problem and should be paid much more attention to.

References

Baskakov, A. P., Mudrechenko, A. V., Bubenchikov, A. M., Starchenko, A. V., Gogolev, A. F., Markovich,

- D. M., 2000. Modelling of U-beam separator. *Powder Technology*, **107**: 84–92.
- Cen, K. F., Qiu, K. Z., Liang, S. R., Yan, J. H., Shen, Y. L., Pan, G. Q., Li, X. D., Ni, M. J., 1998. To characterize two-phase flows around a finned tube using the three-dimensional particle dynamics analyzer (PDA) and numerical calculation. *Powder Technology*, **95**: 129–135.
- De, S., Nag, P. K., 1999. Pressure drop and collection efficiency of cyclone and impact separators in a CFB. *International Journal of Energy Research*, **23**: 51–60.
- Fan, J. R., Zhang, X. Y., Chen, L. H., Cen, K. F., 1997a. Numerical simulation and Experimental Study of two-phase flow in a vertical pipe. *Aerosol Science and Technology*, **27**: 281–292.
- Fan, J. R., Zhang, X. Y., Chen, L. H., Cen, K. F., 1997b. New stochastic particle dispersion modeling of a turbulent particle-laden round jet. *Chemical Engineering Journal*, **66**: 207–215.
- Grant, G., Tabokoff, W., 1975. Erosion prediction in turbomachinery resulting from environmental solid particles. *Journal of Aircraft*, **12**: 471.
- Huber, N., Sommerfeld, M., 1998. Modelling and Numerical calculation of dilute-phase pneumatic conveying of pipe system. *Powder Technology*, **99**: 90–101.
- Zha, X. D., Fan, J. R., Sun, P., Cen, K. F., 2000. Numerical simulation on dense gas-particle riser flow. *Journal of Zhejiang University SCIENCE*, **1**: 29–38.